

A Wind Tunnel Two-dimensional Parametric Investigation of Biplane Configurations

Barcala-Montejano, M.A *, Rodríguez-Sevillano, A.A *, Rodríguez-Rojo, M.E**, Morales-Serrano, S***
 Universidad Politécnica de Madrid, Spain.

miguel.barcala@upm.es, angel.rodriguez.sevillano@upm.es
erguezrojo@gmail.com, sara.moraless@hotmail.com

**Student of Master UPM in Aeronautical Engineering

***Bachelor student UPM of Aeronautical Engineering

Abstract

This paper presents an experimental and systematic investigation about the influence of geometric parameters on biplane configuration (such as stagger, decalage, and gap between upper and lower wing) in aerodynamics parameters. This experimental investigation was developed in a bidimensional approach. Among the unorthodox configurations [1,3,4,5] proposed in new airplane designs, identified in terms of the number and position of lifting-surfaces, the box-wing configuration is a lay-out in which the lifting surfaces (wing and horizontal tailplane) are connected. Theoretical studies about biplanes configurations have been developed in the past [5, 9], but there isn't enough information about experimental wind tunnel data, in the range of low Reynolds number.

An experimental two-dimensional study was presented, as a first step to further tridimensional investigations about feasibility of several solutions. We present a series of experimental data, obtained in a wind tunnel for low Reynolds number values. The box-wing configuration has been employed in a small number of existing UAV, and this is a promising field of actuation applied to new aerodynamics studies and design of unmanned aerial vehicles, and to which the authors have devoted their research efforts for quite a long time now [6, 7 ,9]. The data will be presented in several graphs, such as: C_L vs α , C_D vs C_L , C_L/C_D vs C_L , C_m vs α , $C_L^{1/2}/C_D$ vs C_L , $C_L^{3/2}/C_D$ vs C_L . On the basis of this experimental information, a set of conclusions about the best configurations are proposed. These selected lay-outs will be based on mission criteria (maximum endurance, maximum range, short take-off and landing). Finally, we show the configuration which best accomplishes the aerodynamics criteria.

Notation

C_L \equiv Lift coefficient.

C_D \equiv Drag coefficient.

C_{Di} \equiv Induced drag coefficient.

α \equiv Angle of attack.

$\frac{C_L}{C_D}$ \equiv Lift-to-drag ratio.

C_m \equiv Pitch moment coefficient.

$C_L^{1/2}/C_D$ \equiv Aerodynamic ratio related with maximum range in a jet airplane.

$C_L^{3/2}/C_D$ \equiv Aerodynamic ratio related with maximum endurance in a propeller airplane.

AR \equiv Wing Aspect Ratio.

e \equiv wing span efficiency factor.

V_∞ = Wind tunnel test section freestream velocity.

V_c = Corrected velocity in the wind tunnel test section due to blockage effects.

ε = Correction factor for blockage effects.

A_{wing} = Wing area.

A_{TS} = Test section area.

δ_w = Boundary correction factor.

$\rho \equiv$ air density.
 $A \equiv$ Box-wing wing area. $A = 2 A_{wing}$
 $c \equiv$ wing chord.
 $L \equiv$ Lift force.
 $D \equiv$ Drag force.
 $M \equiv$ Pitching Moment.

1. Introduction

In the last years new aircraft configurations have been studied aiming to achieve improvements in the aircraft performance. “The presently dominant configuration can no longer be improved, making the end of progress”, Torenbeek [11, 12] said.

The main way of improving the aerodynamic behaviour of an aircraft is to decrease its drag force. The latest studies in this field focus on configurations with lower induced drag than the present ones.

Induced drag is the drag due to lift. It is the drag predominant at low speeds. Our work deals with UAS, Unmanned Aerial Systems, in the low Reynolds number regime. This implies low velocities, or low sizes, or both, thus the induced drag constitutes most of the drag. Hence, important achievements could be obtained with a configuration which minimizes induced drag.

Nonplanar wings achieve a reduction of drag compared with planar wings of the same span and lift [4]. There are numerous nonplanar configurations to consider as candidates to be studied as a way of reducing drag. Although, the one which achieves the minimum induced drag for a given lift, span and vertical extent, is the box-wing configuration. This fact is represented by the value of the span efficiency factor, e , as shown in the figure bellow.

$$C_{Di} = \frac{C_L^2}{\pi A R e} \tag{1}$$

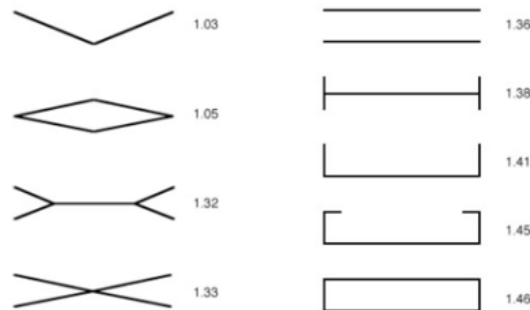


Figure 1: Wing Span efficiencies for various optimally loaded nonplanar systems ($h/b=0.2$). From [1].

Different combinations of geometrical parameters in box-plane configurations lead to different aerodynamic behaviour. A systematic study of these parameters has been carried out aiming at demonstrating the box-wing’s theory, with Prandtl and Munk as main researchers.

A two dimensional model was designed, in which four geometric parameters can be modified: the gap, the stagger, the angle of incidence and the sweep. The gap is the vertical distance between the quarter chord points of each wing. The stagger is the longitudinal distance between the quarter chord points of each wing, positive if the upper wing is forward the lower wing. The incidence is the angle of each wing between a reference position and the flow direction. And the sweep is the angle between the leading edge of the wing and the perpendicular line to the plane symmetry of the airplane.

The model has been tested in a three dimensional wind tunnel. As the study is a two dimensional one, two end plates have been added at both sides of the model, trying to achieve for a two dimensional flow conditions. Geometrical parameters have been changed systematically during the tests. The total aerodynamic forces and moment have been measured in all the cases.

The theoretical studies about box-wing can be resuming in three formulations:

- The minimum induced drag configuration has the same span loading on each wing, and a lift distribution which approaches zero at the midpoint of the vertical planes; the lift distribution in the wings is the addition of a

constant lift distribution and an elliptical distribution [13], [14], [15]. This wing configuration is called the Prandtl's Best Wing System.

- If the lift distribution or circulation is held constant, the total induced drag of the system is unaffected by changes in the longitudinal position of the elements. This theorem was enounced by Munk [16] in 1921, and it is known as Munk's Stagger Theorem. The theorem implies that box-wing design is independent of sweep and stagger if the correct span loading is maintained.
- Finally, the induced drag decreases for increasing non-dimensional gaps [17].

In the present research, it has not been studied the different positions of the wing maintaining the span loading. As an experimental work, all the combinations of parameters have been tested. With changes in stagger and sweep, lift distribution changes, as it does with changes in gap and incidence. Our objective has been to examine the experimental results, aiming to find a confluence between experimental analysis and theoretical studies in further analysis. Helped by Vortex Lattice programs, we will try to establish concordance between the three theoretical points reflected above, and the wind tunnel results.

Because the study is a two-dimensional one, important aspects, as the height to span ratio variation, stability of the system or the structural characteristics are out of consideration. In the hope of carrying out a future research considering these aspects, a model of a box-wing aircraft has been designed.

Height to span ratio variation is the most important design variable for a box-wing aircraft [18]. If a single wing is separated into two wings, with the same total area and span than this wing, maximum induced drag reduction is achieved [19]. That is because aspect ratio has been doubled, and an increase in aspect ratio reduces the induced drag. This reduction goes bigger as the gap increases, because the interference factor between the two wings decreases.

The height to span variation has been taken into account in the design of the model. The model includes planar and box-wing configurations. The planar configuration is a wing with winglet devices at the tips. It is the upper forward wing of the box-wing configuration. The aft lower wing is attached to the first wing and the fuselage, to achieve the box wing configuration. The model has also a removal tail, for being used, if necessary. The wings in the box-wing system have nearly the same span and total area as the monoplane's wing; the lower wing only differs from the upper wing in the winglet segment.

The characteristics of the upper wing, the wing of the monoplane configuration, have been obtained from [20], which deals with the search of optimal nonplanar lifting surfaces. These authors vary a number of wing elements, and use a panel method and a beam finite-element model, helped both by an augmented lagrangian particle swarm optimizer, aiming to solve the multidisciplinary aerostructural optimization problems. They found that, only when aerodynamics are considered, closed lifting surfaces, as box-wing and joined-wing, are the optimal ones, these which minimize the drag. However, when aerostructural optimization is performed, a winglet configuration is found to be optimal, with an overall span constrained, and a wing with a raked wingtip is optimal, with no constrained span.

We have chosen the winglet wing as the planar configuration, because the span is constrained by the dimensions of the wind tunnel where the model will be tested. The wing's dimensions have been calculated based on the dimensions of the mentioned paper.

The box-wing geometric parameters have been chosen in accordance to the conclusion of the experimental study, selecting the confluence of parameters which minimize the drag and the total moment in the arm of the model, and have the highest lift.

As our work is focused on UAS systems, the fuselage and the tail have been designed using other UAS as reference, such as the Outrider or the D1.

The objective of designing a three dimensional model is to compare the aerodynamic responses of the planar configuration and the nonplanar configuration. Moreover, the stability can also be studied. Using this model we would like to determine the advantages and disadvantages between the planar configuration, used nowadays in commercial aircrafts, and the box-wing configuration, the new trend in the aeronautical world.

Furthermore, we would want to make structural studies. According to [21], a 24% lighter aircraft could be designed, using a nonplanar configuration. The Miranda's box-wing configuration [22], covers a minimum induced drag along with structural and stability benefits

The box-wing configuration is the alternative configuration which seems to have better responses than present aircraft design, in the aerodynamic field as well as in the stability and structural fields. Its application for UAS is very advantageous, because in the low Reynolds numbers induced drag is the most important contribution to the total drag. Highest endurance and range could be achieved with this wing configuration.

2. Experimental apparatus

The model consists of **four wings**, two with sweep angle and two without sweep. All of them have been manufactured by a CAD/CAM milling machine, of Necuron material. The airfoil selected has been the **Eppler387**,

appropriate for low Reynolds numbers. The **chord** of the wings is a constant one, with a value of **0.175 m**. The **span** of the wings is **0.140 m**, parameter which is not relevant because we have worked with a two-dimensional flow. The wings have at both sides a **pair of aluminium narrow plates**, which allow changing the incidence during the tests and strengthening the union between the wings and the lateral model plates. They show two holes, one aligned with the quarter chord point of the root chord, and the other one at a distance of a chord from the first one. This second hole permits the change of angle of incidence, rotating the wing around the first hole. Screws have been used to fix the positions. In the lateral plates of the model, three holes have been situated in a straight line. The variation of the incidence of the wing has been achieved by changing the matching between the second hole of the plates in the wing and one of the three holes in the end-plates of the model. The biggest difference of incidence between the upper and lower wing is ± 6 degrees.

The **lateral aluminium plates of the model** have a 1.5 mm width. They assure a two dimensional flow condition during the tests and support the wings, allowing the changes of the geometrical parameters. They present three vertical positions, permitting the variation of the gap in a one and a half chord distance. They also present longitudinal holes which allow the change of longitudinal parameters, such as sweep and stagger. Finally, in some longitudinal positions, additional holes have been made to permit an interval of incidence angle variations.

The model union to the wind tunnel balance is with a sting end which parts from one of the lateral plates (a sting ended connection mounted on one of the lateral plates links the model with the wind tunnel balance). The plate which allows the attachment with the balance represents the fuselage-wing union. The wings with sweep have been moved forward or backwards in this plate to achieve the desired configuration. On the other plate there is no difference in the longitudinal position of the leading edge of the wings.

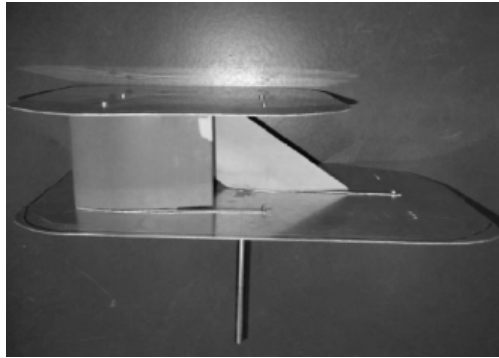


Figure 2: Upper view of the entire test model.

The **wind tunnel** involved in the tests is a low speed open return wind tunnel; it is open on both ends and draws air from the room into the closed test chamber (square section), used for three dimensional tests. It discharges directly to the laboratory, thus the pressure in the tunnel is nearly the atmospheric pressure in the laboratory, preventing blockage problems. The range of the tunnel airspeed is between 0 and 33 m/s. The models have been mounted on one of the tunnel walls, with the balance placed on this lateral position, which allows one degree of freedom; it permits the change of the pitch angle. This **balance gives three forces measurements**, two lift components (with these two components we can calculate pitching moment value), and one drag component.

The lift measure points have longitudinal separation of 0.127 m. The total lift is the addition of both readings. The measures of the lift are negative, so the model had to be placed upside down in the test section. The pitching moment is the result of the difference between the two readings multiplied by the distance between the two points.

The wind tunnel is provided with an **electronic transducer**. This device allows to measure the wind tunnel speed, through the differential pressure gauge between static and total pressure (using Bernoulli equation).

The aerodynamic forces acting on the model are transmitted to the wind tunnel balance, and from there they are recorded by the **data hardware**. This hardware converts analogical signals, corresponding to the measures of the forces, to digital signals. These digital signals are again transmitted to the **data software, Labview3.3.c**, which presents and stores the results on a computer.

3. Experimental procedure

3.1 Wind tunnel corrections

There are two main corrections to be done in the wind tunnel measurements.

First, the blockage effects have to be considered. They are estimated with the ratio of frontal area of the model to the wind tunnel test section cross-sectional area. The ratio resulted has to be lower than the maximum admissible ratio [23]. The wind tunnel test section freestream velocity, V_∞ , is corrected for the blockage effects to give V_c .

$$V_c = (1 + \varepsilon) V_\infty \quad (2)$$

Where ε is the correction factor for blockage effects:

$$\varepsilon = 0.25 \frac{\text{model frontal area}}{\text{test section area}} \quad (3)$$

Secondly, the corrections for the wall interference have to be studied. Wind tunnel walls induced interference can partly be eliminated by applying angle-of-attack corrections. One of the most frequently used corrections is the Glauert Correction Methodology [24]. It is considered to be the classical correction method for wind tunnel tests with fixed wing models. In addition, the angle-of-attack corrections can be found by utilizing other flow theories, like the Heyson and Brooks Correction Methodologies [25, 26], or by experiment.

In the Glauert Correction Methodology the induced angle correction is in the form:

$$\Delta\alpha = \left[\frac{\delta_w A_{wing}}{A_{TS}} \right] C_L \quad (4)$$

The wing area is represented by A_{wing} , A_{TS} is the test section area, C_L is the lift coefficient and δ_w is the boundary correction factor.

The boundary factor, δ_w , is dependent on the test section shape, the ratio of the wing span to tunnel width, and the position of the wing in the test section.

In the present work no correction has been applied. The purpose of the study is to compare the results of each configuration, not to obtain the exact results of each campaign. If in further studies there is the need of higher accuracy, the corrections will be introduced.

3.2 Tested model characteristics

There are five configurations, each of them differing to the rest in the stagger. These configurations have been denominated with a pair of capital letters. The letters represent the type of sweep the wing has, and the stagger of the configuration. The letter ‘‘A’’ represents no sweep, letter ‘‘B’’ represents negative sweep, and letter ‘‘C’’ represents positive sweep. The order of the two letters is also important: the first position indicates that the wing is the upper one, and the second place represents that the wing is the lower one. In the configurations there are always a wing swept and a no swept wing, except for the run with the two wings without sweep. The leading edge of the root chord of the wings with sweep is one chord distance backward or forwards the leading edge of the root chord of the wing without sweep.

The five configurations are represented bellow following this nomenclature. The position in which the model has been attached to the wind tunnel balance is upside down, because the configuration of the balance measures the vertical forces downwards in the direction of the local gravity. Thus, the upper part of the test model is actually the lower part of the wind configuration. Several examples of these configurations are: AA; St=0 / AB; St>0 / AC; St>0 / BA; St<0 / CA; St>0

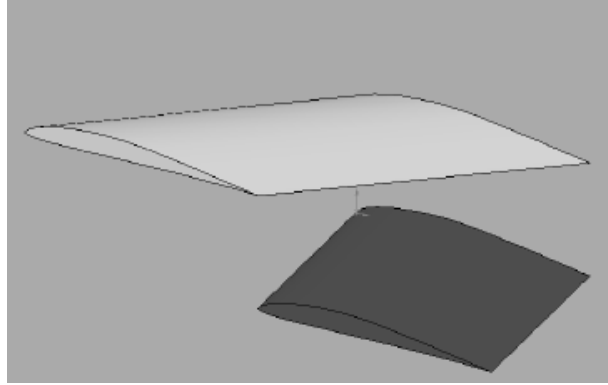


Figure 3: AC configuration; $St > 0$.

The stagger only takes three values: zero and once the chord distance, with negative and positive sign. The positive sign of the stagger corresponds to the cases where the leading edge of the upper wing root chord is forward the leading edge of the root chord of the lower wing.

In the runs of each configuration, the parameters that have been changed are the gap and the incidence of the wings. The variation of the gap has been represented by two values: one chord length and half a chord length. In the nomenclature of the wing configuration, the specification of the gap goes after the two capital letters: "10" represents a gap of a chord distance, and "05" represents a gap of a half chord distance.

With one of the five configurations selected and a gap distance fixed, the difference between the angles of incidence of both wings has been varied. It is specified by adding at the end of the model denomination the value of the relative incidence: ± 6 , ± 3 , 0.

Finally, with one of the five configurations chosen, one gap distance and a relative incidence fixed, the last parameter that has been changed is the angle of attack of the model. This variation has been made by rotating a graduated wheel of the balance; the sting part of the model attached to the balance rotates with this wheel, producing the rotation of the entire model. The angle of attack varies from -15° to $+24^\circ$. This angle has been referred to the upper wing (the lower one in the position into the test section) position at the beginning of the run; if this wing has 3° of incidence in the run, the angle of attack varies between -18° and $+21^\circ$.

Following this order, fifty runs have been made.

One run has been conducted with a reference model, which consist of one wing, not swept and without any incidence angle, making a total of fifty one runs.

Before any test was made, the calibration of the balance was completed. Tests have been run without freestream velocity, to establish the initial conditions of the experiment.

The airspeed velocity for all the runs has been fixed between 20 and 25 m/s, aiming to achieve a Reynolds number of 210000.

The results obtained have been lift, drag and pitch moment. With these forces, the lift, drag and moment coefficients have been calculated.

$$C_L = \frac{L}{\frac{1}{2}\rho V_\infty^2 A}, \quad C_D = \frac{D}{\frac{1}{2}\rho V_\infty^2 A}, \quad C_M = \frac{M}{\frac{1}{2}\rho V_\infty^2 Ac} \quad (5)$$

The moments have been measured in the union axis between the balance and the model. They have been translated to the quarter chord point of the upper wing of the configuration, the lower one in the test position.

4. Results

The variables that have been intended to be studied are:

$$C_{L\max}, C_{D\min}, (C_L/C_D)_{\max}, (C_L^{1/2}/C_D)_{\max}, (C_L^{3/2}/C_D)_{\max}, dC_M/d\alpha, dC_L/d\alpha.$$

The **lift coefficient**, $C_{L\max}$, represents the ability of a wing configuration for giving lift. The more lift it provides, the more weight the aircraft can support, the shorter are the take-off and landing runs, and the higher is the stall velocity. Low values of the **drag coefficient**, $C_{D\min}$, imply less energy that the wing configuration loses in its interaction with the flow. Lower loss of energy allows bigger endurance and range of the aircraft provided with this wing configuration.

High values of the **aerodynamic efficiency**, $(C_L/C_D)_{m\acute{a}x}$, lead to more efficient flights. In a jet airplane, the maximum value of this ratio corresponds to a maximum endurance; in a propeller aircraft, the maximum corresponds to a maximum range.

The maximum value of the variable $(C_L^{1/2}/C_D)_{m\acute{a}x}$ represents, in a jet airplane, the aerodynamic flight condition for maximum range.

The maximum value of the variable $(C_L^{3/2}/C_D)_{m\acute{a}x}$ represents, in a propeller aircraft, the aerodynamic flight condition for maximum endurance.

Six relationships between the variable parameters have been established, in order to easily understand the behaviour of the model. The six scenarios have been examined plotting up the curves of the following pair of variables: $C_L - \alpha$; $C_D - C_L$; $C_L/C_D - C_L$; $C_M - \alpha$; $C_L^{1/2}/C_D - C_L$; $C_L^{3/2}/C_D - C_L$.

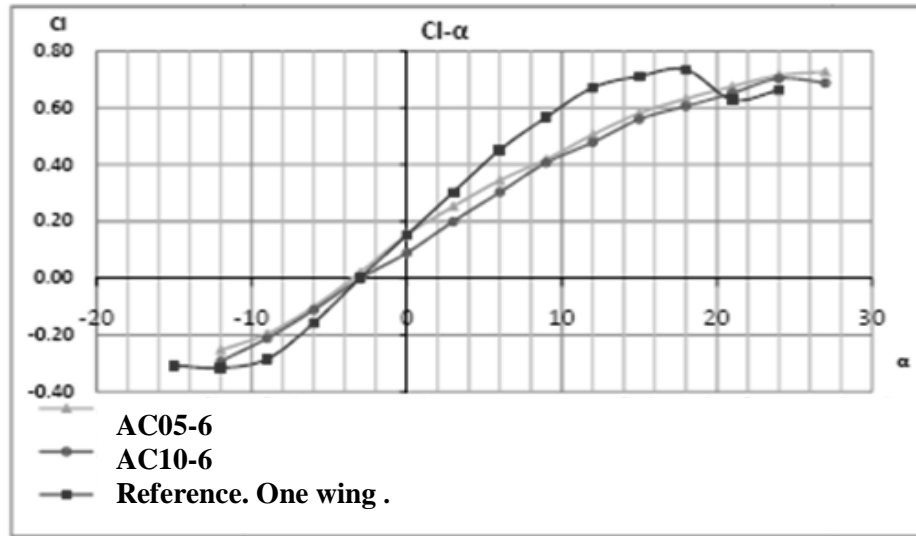


Figure 4: Lift coefficient curves.

For each scenario, the following conclusions have been obtained:

1. Relative incidence and stagger have been maintained constant; the gap changes. The bigger the gap is, the better the results obtained for all the variables implied.
2. Relative incidence and gap have been maintained constant; the stagger changes. The better behaviour has been observed for positive staggered configurations, with the lower wing with positive sweep (Configuration AC). The non staggered configuration AA, has achieved the best results in jet aircraft range coefficient, propeller aircraft endurance coefficient, and aerodynamic efficiency coefficient. The configuration with minimum slope of the moment coefficient has been the AC configuration.
3. The stagger and gap have been maintained constant; the relative incidence changes. The change of the incidence angle has not affected strongly the performance of the wing configuration.
4. The stagger has been maintained constant; the relative incidence and gap change. In almost all cases, the configuration with the best behaviour has showed a gap distance of once the chord distance. The change of the incidence angle has followed a more arbitrary pattern.
5. The relative incidence has been maintained constant; the stagger and gap change. The configurations with better performances have been AA10 and AC10. Only in the analysis of the moment coefficient slope, the half chord gap has achieved better results than the one chord gap. That is because the moments in the quarter chord point of the upper wing will be lower if the wings are closer.
6. The gap has been maintained constant; the relative incidence and stagger change. The configurations AA and AC have been the ones with better performance results. With respect to the incidence angle, there has not been a clear enough pattern to establish.
7. The maximum **lift coefficient slope** has been examined. The configuration with the highest slope has been the AA10-3 configuration.

Finally, **one run with one wing, without sweep and incidence, was conducted.** In all the cases considered, the planar configuration has showed worse behaviour than the nonplanar configuration, excluding the slope of the lift coefficient curve. It has a higher value of the slope of the lift coefficient versus angle of attack curve. But the stall appears earlier, at lower angles of attack, in this configuration than in the nonplanar systems.

5. Conclusions

In this section, we present the main conclusions related to:

$$C_{Lmax}, C_{Dmin}, (C_L/C_D)_{max}, (C_L^{1/2}/C_D)_{max}, (C_L^{3/2}/C_D)_{max}, dC_M/d\alpha, dC_L/d\alpha.$$

The maximum values of the **lift coefficient**, versus the angle of attack, have been obtained for the configurations AC10+3, AC050, AC100 and AC05+3.

The minimum values for the **drag coefficient** have been observed in the configurations AA10-3 and AC10+3.

The maximum values of **aerodynamic efficiency**, which represents the maximum range in propeller aircraft and maximum endurance in jet airplanes on aircraft, have been obtained for the configurations AA100 and AA10-3.

The maximum values for the relation between the lift and drag coefficient which maximizes the jet aircraft range parameter $(C_L^{1/2}/C_D)$, have been given for the configurations AA100 and AA10-3.

The ratio which maximizes the endurance in propeller aircraft $(C_L^{3/2}/C_D)$ has been found to be maximum in the configurations BA10-6 and AA100.

The **pitching moment coefficient** has been referred to the quarter chord point of the upper wing root, instead of being referred to the aerodynamic centre. Even though, conclusions for the coefficient curve slope have been obtained: the lower the curve slope is the lower the pitch moment will be, in any point of the configuration. Hence, the better behaviour the configuration will have to longitudinal perturbations. The configurations with the lowest slopes in the graphs of moment coefficient versus angle of attack have been AC05+6 and AC05+3.

Finally, the configuration with a highest **lift coefficient slope** has been the AA10-3 configuration.

We can conclude that the configuration without stagger, AA, and a one chord gap, AA10, presents good performance behaviour in the maximization of range and endurance of propeller and jet airplanes. The configuration AC shows good results for maximum lift coefficient and minimum drag coefficient, in addition to the best answer in the minimization of the pitching moment coefficient slope.

The predominant gap value is the one chord value, though the half chord gap obtains better results in the moment coefficient slope.

With regards to the relative incidence, clear conclusions cannot be obtained yet.

With the aim of designing a **three dimensional model**, the **AC10** configuration has been chosen. Despite the worse results in endurance, range and efficiency, it has been observed that these results are not too far from the best ones. The advantages of this configuration versus the biplane are related to the stability and the higher maximum lift coefficient. It also presents a minimum drag coefficient, as the biplane configuration. Another advantage, not related with the previous variables, is the higher pitching control capability of this wing configuration. A configuration like the AC could have control during flight without additional control surfaces, as the horizontal and vertical stabilizers. The aft wing could act as the elevator. In the lateral planes, union between both wings, there could be slats which act as rudders. The inclusion of the controls in the wing would save a lot of weight.

As it has already been mentioned, the three dimensional model **includes two configurations**, the planar configuration with the upper wing and tail, and the box-wing configuration, with upper and lower wing and without tail. The design of the three dimensional model is based on box-wing of UAS in service, such as the Outrider and the D1. The upper forward wing design is funded on a research paper by [20].

With this model we intent to undertake a further study of the box-wing configuration, comparing it with the nowadays wing configuration. We will try to establish the advantages and disadvantages between the aerodynamic response of the wing with winglets and the box-wing. We will also like to obtain the stability analysis of both configurations, to study the differences in this field.

Finally, in future studies we will deal with the structural part of the problem, analysing if the box-wing configuration has structural advantages against the planar configuration.

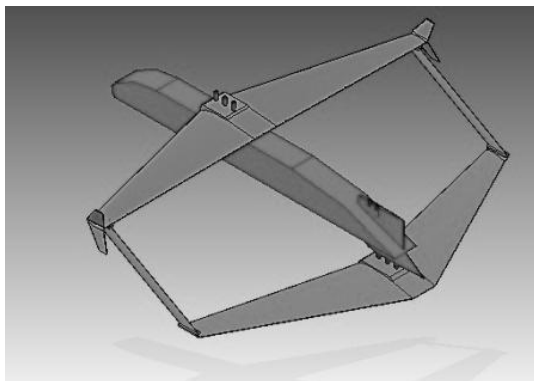


Figure 5: Box-wing configuration

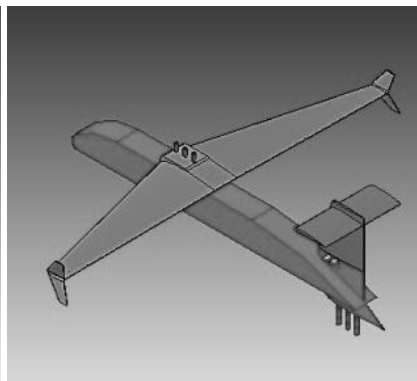


Figure 6: Planar configuration

References

- [1] Kroo, Ilian. Drag Due to Lift: Concepts for Prediction and Reduction. *Annu. Rev. Fluid Mech.* 2001. 33:587–617. 2000 by Annual Reviews.
- [2] Mueller, T. J., & DeLaurier, J. D. (2003). Aerodynamics of small vehicles. *Annual Review of Fluid Mechanics* , 35, 89-111.
- [3] Innovations in Aeronautics. Kroo, Ilian. AIAA 2004-0001, Reno : s.n., 2004, AIAA.
- [4] Kroo, I. Nonplanar Wing Concepts For Increased Aircraft Efficiency. VKI Lecture Series on Innovative Configurations and Advanced Concepts for Future Civil Aircraft. June 6-10, 2005.
- [5] Prandtl, L. Induced drag of multiplanes. NACA TN 182, 1924.
- [6] Barcala, M, Cuerno-Rejado, C., del Giudice, S., Gandía-Agüera, F., Rodríguez-Sevillano, A.A.. Experimental Investigation on Box-Wing Configuration for UAS. 26th Bristol International Unmanned Air Vehicle Systems Conference. University of Bristol, UK. 11 - 13 April 2011.
- [7] Gandía-Agüera, F. Rodríguez-Sevillano, A. A. Barcala-Montejano, M.A. Holgado-Vicente, J.M. Systems integration in a UAS design. An example of undergraduate students' tasks. 2011 IEEE Global Engineering Education Conference (EDUCON). IEEE Engineering Education 2011. Learning Environments and Ecosystems in Engineering Education. Amman 4-6 April 2011. ISBN 978-1-61284-641-5. Print ISBN 978-1-61284-642-2. DOI: 10.1109/EDUCON.2011.5773178. Pag 470-476.
- [8] Gall, P.D. An experimental and theoretical analysis of the aerodynamic characteristics of a biplane-winglet configuration. NASA TM 85815, 1984.
- [9] Barcala-Montejano, M.A., Gandía-Agüera, F., Rodríguez-Sevillano, A.A., Crespo-Moreno, J., Pérez-Álvarez, J., Gómez-Pérez, J.P., Gómez-Pérez, I. The application of Rapid Prototyping in the design of an UAV. 27TH CONGRESS OF THE INTERNATIONAL COUNCIL OF THE AERONAUTICAL SCIENCES (ICAS-2010), Nice-France 19-24 September 2010. ISBN 978-0-9565333-0-2.
- [10] Austin, R. Unmanned Aircraft Systems. UAVS Design, Development and Deployment. Chichester, Reino Unido, John Wiley & Sons Ltd. 2010.
- [11] Torenbeek, E. (2005). Blended-wing-body and all wing airliners. In 8th European Workshop on Aircraft Design Education.
- [12] Torenbeek, E. (1982). Synthesis of subsonic airplane design: an introduction to the preliminary design of subsonic general aviation and transport aircraft, with emphasis on layout, aerodynamic design, propulsion and performance. Kluwer Academic Pub.
- [13] Prandtl, L. (1924). Induced drag of multiplanes.
- [14] Von Karman, T., & Burgers, J. M. (1935). General aerodynamic theory-perfect fluids. *Aerodynamic theory*, 2, 308.
- [15] Frediani, A., Gasperini, M., Saporito, G., & Rimondi, A. (2003). Development of a Prandtlplane aircraft configuration. In *Proceedings of the 17th AIDAA Congress, Roma, Italy* (pp. 2263-2276).
- [16] Munk, M. M. 'The Minimum Induced Drag of Aerofoils,' NACA Rept. 121, 1921.
- [17] Frediani, A. (2005). The Prandtl Wing. Lecture Series on Innovative configurations and advanced concepts for future civil aircraft, Von Karman Institute, ISBN, 2-930389.
- [18] Khan, F. A., Krammer, P., Scholz, D. (2010). Preliminary aerodynamic investigation of box-wing configurations using low fidelity codes. DGLR: Deutscher Luft-und Raumfahrtkongress.
- [19] Raymer, D. P. (1992). *Aircraft Design: A Conceptual Approach*. Washington DC: American Institute of Aeronautics and Astronautics.

- [20] Jansen, P. W., Perez, R. E., & RA Martins, J. R. (2010). Aerostructural optimization of nonplanar lifting surfaces. *Journal of Aircraft*, 47(5), 1490-1503.
- [21] Wolkovitch, J. (1986). The joined wing-An overview. *Journal of Aircraft*, 23(3), 161-178.
- [22] Miranda, L. (1972). Boxplane configuration, conceptual analysis an initial experimentation. LR 25180, Lockheed California.
- [23] Barlow, J. B., Rae, W. H., & Pope, A. (1999). Low-speed wind tunnel testing.
- [24] Glauert, H. (1933). Wind Tunnel Interference on Wings, Bodies and Airscrews.
- [25] Heyson, H. H., "Rapid Estimation Of Wind Tunnel Corrections With Applications To Wind Tunnel And Model Design," NASA TN D-6416.
- [26] Brooks, T. F., and C. L. Burley, C. L., "A Wind Tunnel Wall Correction Model for Helicopters in Open, Closed, and Partially Open Rectangular Test Sections," NASA TM to be published August 1996.